J Mater Sci (2011) 46:6823–6829
DOI 10.1007/s10853-011-5641-2

The influences of firing temperatures and excess PbO on the crystal structure and microstructure of $(Pb_{0.25}\ Sr_{0.75})TiO_3$ ceramics

Rattiphorn Sumang · Theerachai Bongkarn

Received: 17 December 2010 / Accepted: 16 May 2011 / Published online: 1 June 2011

Abstract Polycrystalline samples of $(Pb_{0.25}Sr_{0.75})TiO_3$ (PST75) were prepared by the solid-state reaction method. The effects of firing temperatures and excess PbO on PST75 ceramics were investigated. The PST75 was calcined between 600 and 1000 °C for 3 h and the sintering temperature ranged between 1050 and 1250 °C for 2 h. The optimized calcination and sintering conditions were identified as 950 and 1250 °C, respectively. The lattice parameter *c* increased, while the lattice parameter *a* decreased with increased firing temperatures. The average particle size and average grain size increased with increased firing temperatures. After the addition of PbO—excess 0, 1, 3, 5, and 10 wt%—in the PST75 samples, the lattice parameter *a* decreased. The average particle size and the average grain size increased with the increase of PbO. The porous microstructure slightly decreased with an increasing amount of PbO—up to 3 wt%—then slightly increased with the higher excess PbO. The density was improved by adding 3 wt% of excess PbO. A low dielectric loss was observed from the 3 wt% excess PbO sample.

Introduction

$(Pb_xSr_{1-x})TiO_3$ (PST) is a complete solid solution of $PbTiO_3$ (PT) and $SrTiO_3$ (ST). Nomura and Sawada [1] studied the PT:ST solid solution system and found an easy formation for a good homogeneous composition. With the addition of ST to PT, the Curie temperature decreases linearly and the phase transition from tetragonal to cubic occurs at $x \approx 0.65$ at room temperature. Somiya et al. [2] studied the PST solid solution with $0.7 < x < 0.8$. These are the most suitable for microwave applications due to their high dielectric constant and extremely high dielectric tenability of 70% under 2 kV/cm at 1 kHz with a very low dielectric loss value of less than 0.001 [3].

Various fabrication techniques such as sol–gel [3, 4], coprecipitation [5], complex polymerization [6], and the precursor solution [7] have been used to study PST ceramics. All these methods use high-purity inorganic or organic chemicals with a homogeneity and precise composition as starting materials but the production costs are high with only small quantities synthesized. The conventional solid-state reaction method is more economical for large batch processing of these ferroelectric materials [8, 9]. A previous work showed that PST ceramics could be prepared by conventional methods using high sintering temperatures above 1200 °C [4, 10, 11]. This created problems with vaporization of PbO during sintering because of the low melting point of PbO, which is about 850 °C. This can cause lead deficiency which may produce large pores in the microstructure and have a subsequent effect on densification. The addition of excess PbO is one of the techniques developed to counteract this problem. For example, the optimum density of Bi-doped PT [12], PBZ [13], PBT [14], PZT [15] ceramics, can be improved by the addition of excess PbO. Therefore, the effect of firing temperatures and excess PbO on the crystal structure and microstructure of $(Pb_{0.25}Sr_{0.75})TiO_3$ ceramics synthesized by a solid-state reaction method were investigated in this study.

Experimental

Ceramic composition of $(Pb_{0.25}Sr_{0.75})TiO_3$; PST75 was prepared by the solid-state reaction method. Lead oxide

R. Sumang · T. Bongkarn (✉)
Department of Physics, Faculty of Science, Naresuan University, Phitsanulok 65000, Thailand
e-mail: researchcmu@yahoo.com

(99.9% PbO), strontium carbonate (99% $SrCO_3$), and titanium oxide (99.5% TiO_2) powders were used as starting materials. The starting powders were weighed in the required stoichiometric ratio and then ball-milled in ethanol for 24 h. After the drying process, the mixed powders were calcined from 600 to 1000 °C with a 5 °C/min heating/cooling rate for 3 h to discover the optimum calcinations temperature. The calcined powders were mixed with 4 wt% binder and then ball-milled again in ethanol for 24 h. Subsequently, the calcined powders were pressed into disks with a diameter of 15 mm at a pressure of 80 MPa. The disk samples were then sintered from 1050 to 1250 °C for 2 h to discover the optimum sintering temperature. In order to compensate for the PbO loss during the process of calcination and sintering, excess PbO was added. The excess PbO was subdivided into 0, 1, 3, 5, and 10 wt% at calcination and sintering temperatures of 950 and 1250 °C, respectively.

The reactions of the uncalcined PST75 powders taking place during heat treatment were investigated by differential thermal analysis (DTA) and thermo gravimetric analysis (TGA). The structure phase of the calcined powders and sintered ceramics was identified using an X-ray diffractometer (XRD). The typical size of the crystallites was determined from scanning electron microscopy (SEM). The apparent density of the samples was measured by the Archimedes method with distilled water as the fluid medium. Silver electrodes were constructed on two major surfaces of the polished samples and dielectric measurements were performed using a LCR meter (Agilent 4263B).

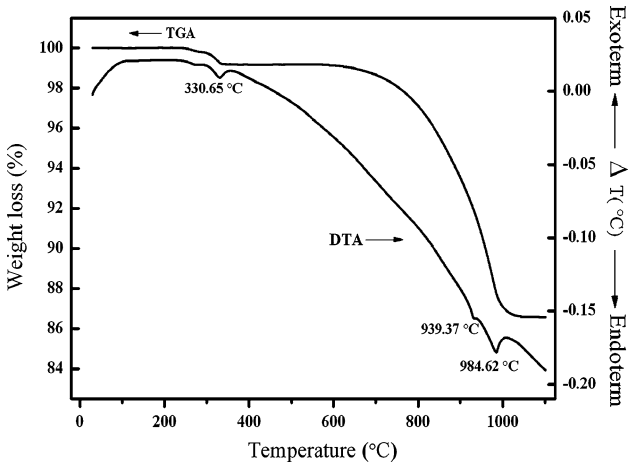

Fig. 1 The DTA–TGA curves for the mixture of PbO, $SrCO_3$, and TiO_2 powders

Results and discussion

The DTA–TGA simultaneous analysis of the powders mixed in stoichiometric proportions of PST75 is displayed in Fig. 1. The sharp decrease curve of the TGA, between 250 and 320 °C, indicated a major weight loss due to the process of getting rid of the left over burned plastic during the ball milling and related to a small endothermic peak at 331 °C in the DTA curve. The second weight loss was

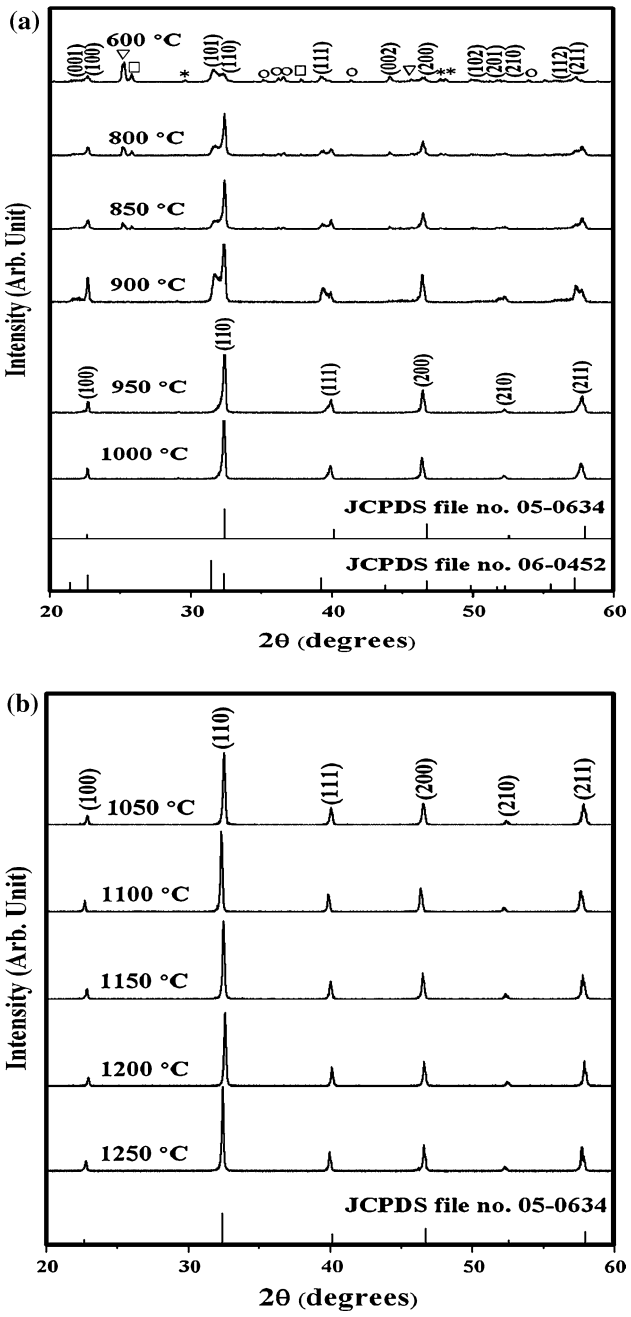

Fig. 2 XRD pattern of PST75 **a** calcined powders and **b** sintered ceramics with different firing temperatures (*asterisk* PbO), (*inverted triangle* $SrCO_3$), (*square* TiO_2), and (*circle* TiO)

observed above 600 °C, which related to the endothermic peak at 939 and 985 ° on the DTA curve. These temperatures caused many chemical reactions between the PbO, $SrCO_3$, and TiO_2. From previous works reported, synthesizing pure $PbTiO_3$ based on the solid-state reaction between PbO and TiO_2 typically occurs at temperatures higher than 630 °C [16], while the pure perovskite phase of $SrTiO_3$ is produced by the solid-state reaction between $SrCO_3$ and TiO_2 at temperatures above 1300 °C [17]. Chen et al. [18] prepared pure PST powders via the solid-state reaction method by calcining at 900 °C for 2 h. Therefore, the reaction between PbO, $SrCO_3$, and TiO_2 of PST75 should begin at a temperature higher than 600 °C but not greater than 1300 °C. These data were used to define the range of calcination temperatures.

The XRD patterns of PST75 calcined powders and sintered ceramics at various temperatures are shown in Fig. 2a, b. The XRD pattern shows a major X-ray reflection peak in the perovskite PST75 phase, indicating the polycrystalline nature of the powder with (110) as the major peak. For the powders calcined at <950 °C, the index of the tetragonal structure matched JCPDS file number 06-0452 [19] and an X-ray peak of precursors (PbO, $SrCO_3$) and impurities (TiO_2, TiO) appeared. The pure cubic perovskite phase was discovered in powders calcined ≥950 °C, which were matched with JCPDS file number 05-0634 [20] and earlier reports [9, 10]. Crystallinity of the calcined powders was improved by increasing the calcination temperature, as indicated by the increase in intensity of the X-ray diffraction peak. The relative amounts of the perovskite phase were calculated by measuring major peak intensities of the perovskite phase. The percentage of perovskite is described by the following equation:

$$\%\ \text{perovskite phase} = \left(\frac{I_{\text{perov}}}{I_{\text{perov}} + I_{\text{PbO}} + I_{\text{SrCO}_3} + I_{\text{TiO}_2} + I_{\text{TiO}}}\right) \times 100 \qquad (1)$$

This well-known equation is widely employed in the preparation of complex perovskite structure materials [9, 21]. I_{perov}, I_{PbO}, I_{SrCO_3}, I_{TiO_2}, and I_{TiO} refer to the intensity of the (101) perovskite peak and the intensities of the highest PbO, $SrCO_3$, TiO_2, and TiO peaks, respectively.

The percentage of the perovskite phase of the PST75 calcined powders was increased from 10 to 96 when the calcination temperature increased from 600 to 900 °C. When increasing the calcination temperature above 950 °C, the percent of the perovskite phase of the samples reached a hundred percent, Table 1. The *a*-, *c*-axis lattice constants of PST75 calcined powders at different temperatures were calculated from the (001)/(100) and (002)/(200) XRD peaks and are shown in Fig. 3. When the calcined temperatures increased, the *a*-axis parameter of the tetragonal structure increased whereas the *c*-axis parameter

Table 1 % perovskite phase, lattice parameter, unit cell volume, average particle size, average grain size, density, shrinkage, and dielectric properties of the PST75 with different firing temperatures

Calcination temperature (°C)	Calcined powder				Sintering temperature (°C)	Sintered ceramic					
	Perovskite phase (%)	*c*/*a* ratio	Unit cell volume (Å^3)	Average particle size (μm)		Lattice parameter *a* (Å)	Average grain size (μm)	Density (g/cm^3)	Shrinkage (%)	Dielectric constant at T_{room}	Dielectric loss at T_{room}
600	10	1.051	63.36	0.12	1050	3.9040	0.30	5.78	3.3	768	0.67
800	52	1.050	62.73	0.14	1100	3.9032	0.42	5.88	5.3	1704	3.53
850	64	1.049	62.70	0.17	1150	3.9016	0.50	5.92	8.6	1743	2.11
900	96	1.047	62.48	0.21	1200	3.8984	0.57	5.94	10.6	1914	1.17
950	100	1.000	59.81	0.24	1250	3.8960	0.59	5.99	13.3	1930	0.39
1000	100	1.000	59.03	0.38							

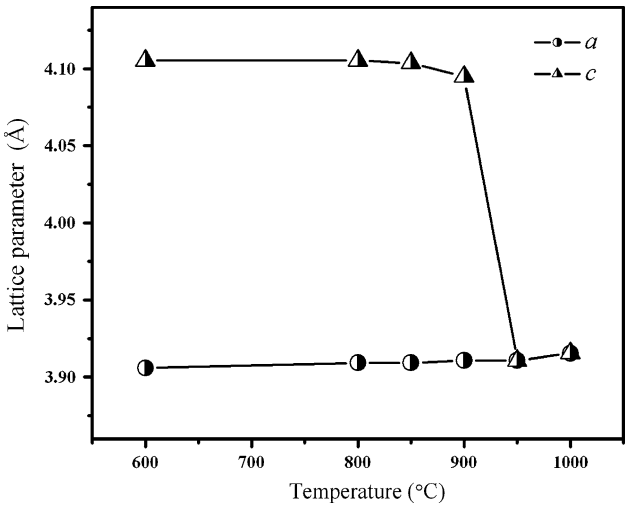

Fig. 3 Lattice parameters of PST75 powders at different calcination temperatures

decreased. The *c/a* ratio and unit cell volume of PST75 decreased with increasing calcined temperatures, as listed in Table 1. In Fig. 2b, the sintered pellets show a pure perovskite phase. The diffraction patterns of PST75 could be indexed with respect to a cubic structure. The *a*-axis lattice constantly decreased with increased sintering temperatures, see Table 1. These indicate that the calcination and sintering temperatures have a direct bearing on the phase formation and lattice parameters.

Figure 4a, b shows SEM photomicrographs of PST75 calcined powders at different temperatures. In general, the particles have a spherical morphology. The average particle size increased from 0.12 to 0.38 μm, when the calcination temperature was increased from 600 to 1000 °C, Table 1. Figure 4c, d shows the microstructure of PST75 ceramics at different sintering temperatures. It was found that increasing sintering temperatures helped grain size growth, Table 1. A similar result was found in Nb-doped PZT and $Pb(Zr_{0.44}Ti_{0.56})O_3$ ceramics [22, 23]. A porous microstructure with a small grain size was observed in the PST75 sintered at 1050 °C. When sintering temperatures increased from 1050 to 1250 °C, the porosity of the PST75 ceramics decreased. However, when the sintering temperature was higher than 1250 °C, the PST75 ceramics became very fragile.

The densities and shrinkage of the PST75 ceramics are listed in Table 1. The density and shrinkage increased with increased sintering temperatures, and the maximum value was 5.99 g/cm^3 and 13.3% obtained from ceramics sintered at 1250 °C.

The dielectric constant and dielectric loss of PST75 sintered ceramics as a result of temperature are listed in Table 1. The dielectric constant of the samples increased when sintering temperatures increased from 1050 to 1250 °C. The dielectric loss increased at first and then dropped as the sintering temperature >1100 °C.

To compensate for PbO loss from evaporation during calcination and sintering, some excess PbO is usually added during the batch preparation. The batch is then

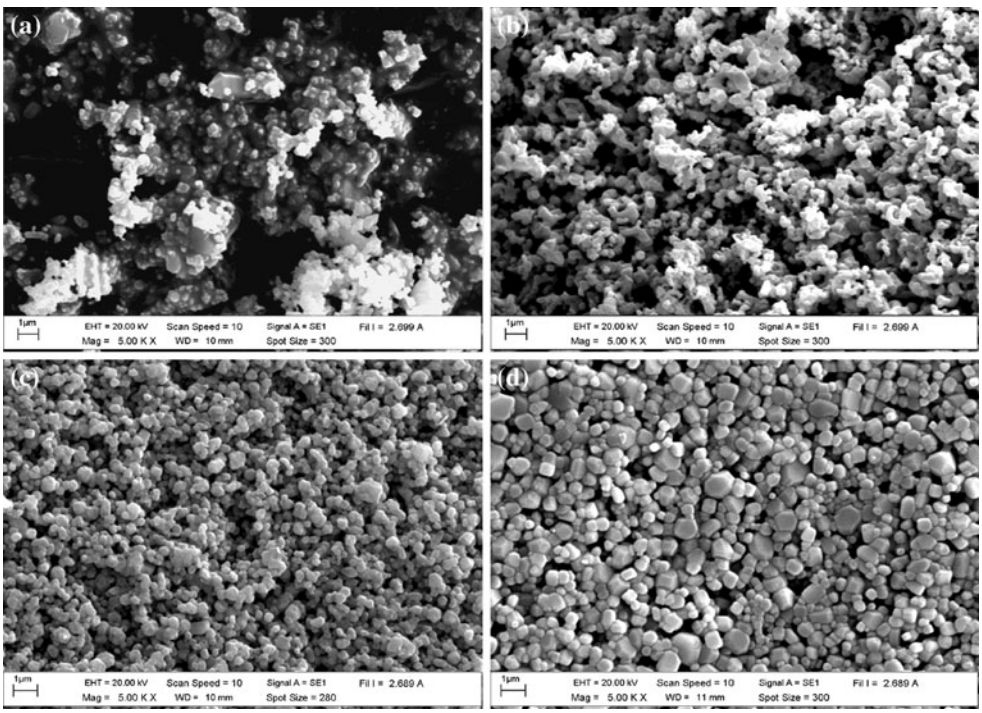

Fig. 4 SEM photomicrographs of PST75 at different firing temperatures: **a** 600 °C and **b** 950 °C of calcined powders, **c** 1050 °C and **d** 1250 °C of sintered ceramics

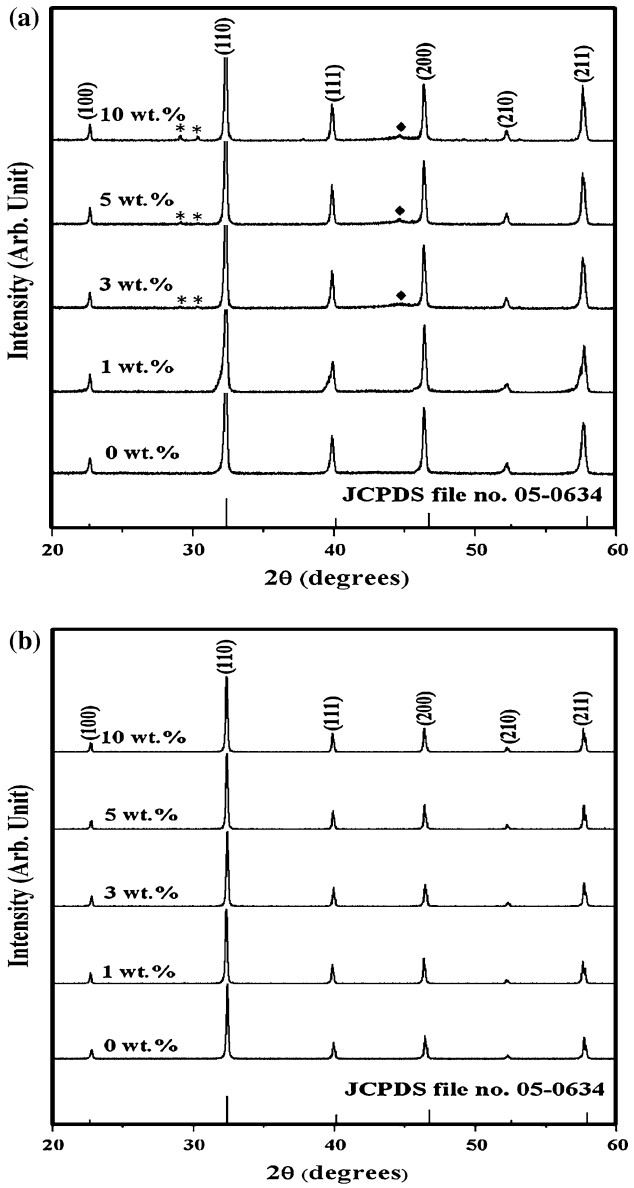

Fig. 5 XRD pattern of PST75 **a** calcined powders and **b** sintered ceramics with different amounts of excess PbO (*asterisk* PbO) and (*diamond* PbO_2)

calcined and sintered at 950 and 1250 °C, respectively. The X-ray diffraction patterns of PST75 calcined powders, containing different amounts of PbO, are shown in Fig. 5a. The crystal structure of the PST75 system was proposed as a cubic phase. The impurity phase of PbO and PbO_2 was found in the ≥3 wt% excess PbO sample. The impurity phases occurred because of too much lead for the proper reaction during calcinations [13, 14]. The percentage of the perovskite phase decreased from 100 to 92 when excess PbO was higher than 1 wt%, see Table 2. The impurity phase was not obtained in any of the ceramics samples, see Fig. 5b. This indicated that the excess PbO exceeded that required to maintain compositional control (assumed) in the PST75 powders and was eliminated from the sample by volatilization during sintering at 1250 °C. The perovskite phase in the ceramics reached a hundred percent in all samples. The lattice parameter *a* of PST75 in the calcined powders and sintered ceramics decreased from 3.9159 to 3.9127 Å and 3.8960 to 3.8864 Å, when increasing excess PbO from 0 to 10 wt%, as listed in Table 2. In the case of the $PbTiO_3$, the sample deficient in PbO exhibited an increase of lattice parameter *a* [24]. The decrease of lattice parameter *a* in this study indicated that the excess PbO was utilized to compensate for PbO-volatility.

The SEM photomicrographs of PST75 calcined powders with various PbO excess are shown in Fig. 6a–c. These powders exhibited an almost spherical morphology and agglomeration. The average particles size increased from 0.24 to 0.59 μm with increased PbO content from 0 to 10 wt%, see Table 2. Figure 7a–c reveals the SEM photomicrograph of PST75 sintered pellets. The grain growth of the PST75 continuously increased with increased excess PbO, changing from 0.59 to 0.76 μm, as listed in Table 2. The PbO may be combined into the ceramics and therefore less liquid phases exist in the grain boundaries. This would hinder the grain growth [14]. A porous microstructure was also found on the surface of the samples without (0 wt%) and with 1 wt% PbO content. With the addition of 3 wt% excess PbO, the porosity decreased, due to a liquid phase

Table 2 % perovskite phase, lattice parameter *a*, average particle size, average grain size, density, and dielectric properties of the PST75 samples with different excess PbO contents

Excess PbO (wt%)	Calcined powder			Sintered ceramic				
	Perovskite phase (%)	Lattice parameter *a* (Å)	Average particle size (μm)	Lattice parameter *a* (Å)	Average grain size (μm)	Density (g/cm^3)	Dielectric constant at T_{room}	Dielectric loss at T_{room}
0	100	3.9159	0.24	3.8960	0.59	5.99	1930	0.39
1	100	3.9151	0.26	3.8919	0.61	6.01	1975	0.33
3	97	3.9143	0.38	3.8917	0.63	6.26	2325	0.08
5	93	3.9135	0.47	3.8903	0.64	5.78	2457	0.19
10	92	3.9127	0.59	3.8864	0.76	5.75	2242	0.20

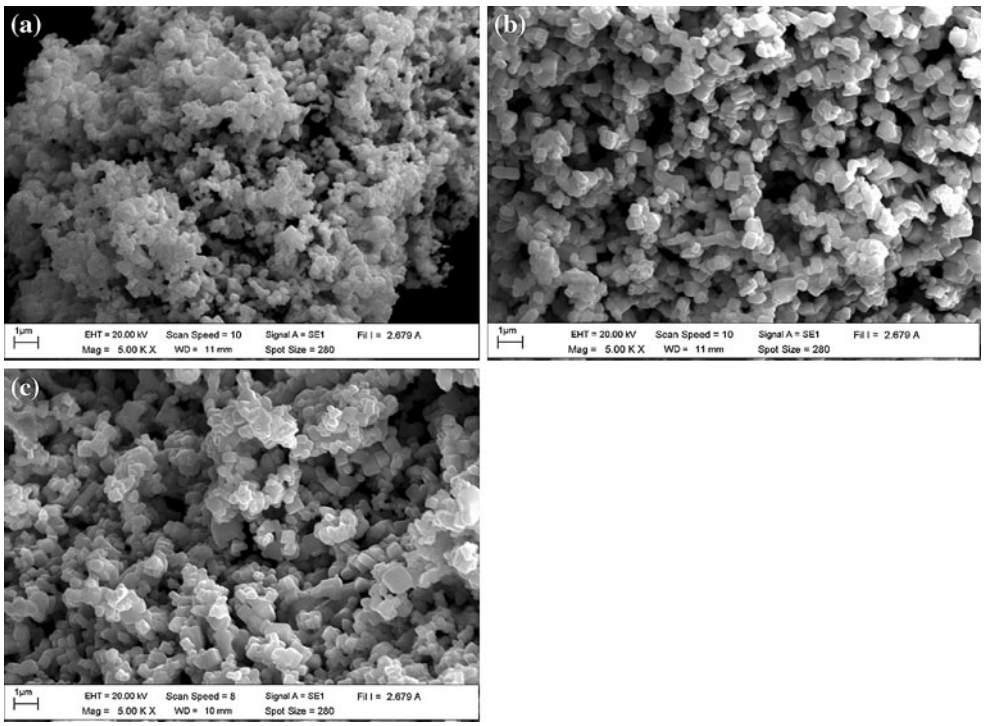

Fig. 6 SEM photomicrographs of PST75 made from starting with different excess PbOs: **a** 0 wt%, **b** 3 wt%, and **c** 5 wt% of calcined powders

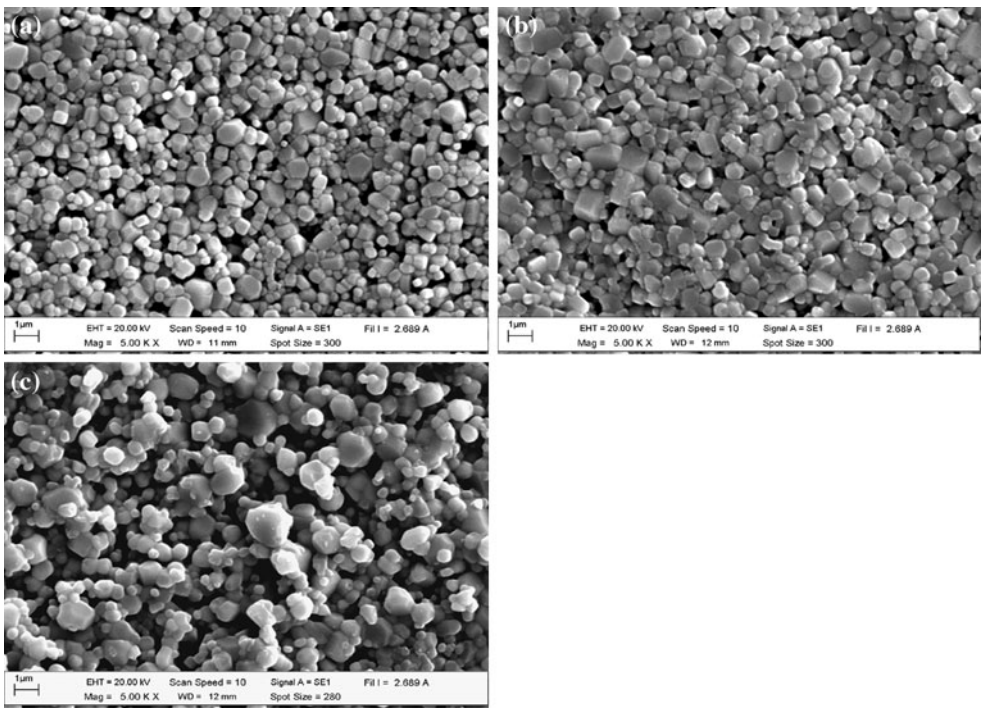

Fig. 7 SEM photomicrographs of PST75 made from starting with different excess PbOs: **a** 0 wt%, **b** 3 wt%, and **c** 5 wt% of sintered ceramics

which formed between the perovskite grains. The porosity increased with an increase of excess PbO. This could be caused by the loss of PbO from the compact pellet which increased its porosity.

The densities of the PST75 ceramics are listed in Table 2. The density increases with increased PbO, reaches a maximum value at 3 wt% excess PbO, and slightly decreases above >3 wt% excess PbO. The density results can be

correlated to the microstructure since the high density for 3 wt% excess PbO samples showed high degrees of close grain packing, whereas the low density of the sample with >3 wt% excess PbO contained many pores. Thus, the porosity of the samples has a marked effect on density. The increases and decreases in the densities of the PST75 ceramics are due to the degree of porosity. The density and porosity depend on the amount of PbO in the liquid phase. In the presence of excess PbO, the densification of the samples takes place by a rapid rearrangement of the particles surrounded by the liquid phase. This process becomes more intense if a sufficient liquid phase is present to allow an easy rearrangement of the grains. Consequently, the densification should be proportional to the amount of liquid PbO. In this study, the amount of liquid PbO was not enough to fill in the pores of the sample without excess PbO (0 wt%) and with excess PbO 1 wt% and appeared on the porous microstructure of the surface of these samples. When the excess PbO was raised to 3 wt%, the effect of decreasing porosity concentration resulted in higher densification. However, a large amount of the PbO liquid phase can produce an initial rapid densification but a lower final density because of void formation due to PbO evaporation. As a consequence the porosity of the pellet increases [12, 25]. In this study, the reduction in density for the 5 and 10 wt% samples is consistent with an excessive amount of PbO in these samples. In the previous study, excess PbO 1 wt% was added to the Pb-based samples (PBZ, PBT, PCT) to obtain a higher densification [13, 14, 26]. In this study, the calcination and sintering were performed at a higher temperatures so a higher excess PbO content (3 wt%) was added in the PST samples to compensate for the vaporization of PbO.

The dielectric constant and dielectric loss of the PST75 ceramics with various excess PbO content are listed in Table 2. The dielectric constant increased with an increased PbO until 5 wt% and then decreased with higher excess PbO. However, the lowest dielectric loss was observed from the 3 wt% excess PbO samples. The dielectric constant and dielectric loss of the excess PbO samples (Table 2) were higher and lower than the samples without excess PbO (Table 1). This indicated that the electrical properties of lead-containing ceramics produced by the solid-state reaction method can be improved by the addition of excess PbO.

Conclusions

Firing temperatures and excess PbO have a strong influence on the crystal structure, microstructure, and lattice parameter of PST75 ceramics. The optimal calcination and sintering conditions were found to be 950 and 1250 °C, respectively. The PST75 powders calcined below <950 °C were indexed with a tetragonal structure, while the pure cubic perovskite phase was discovered in powders calcined at ≥950 °C. For the ceramic samples, the lattice parameter *a* decreased while grain size increased with increasing sintering temperatures. The maximum density of the ceramics was discovered in the pellets sintered at 1250 °C. Furthermore, the particle size and average grain size increased with an increase of excess PbO. Appropriate amounts of the liquid phase can decrease porosity. The density can be improved by adding 3 wt% of excess PbO.

Acknowledgments This study was financially supported by the Thailand Research Fund (TRF), Commission on Higher Education (CHE) and The Royal Golden Jubilee Ph.D. Program. The authors wish to thanks the Science Lab Center, Faculty of Science, Naresuan University for supporting facilities. Thanks are also given to Mr. Don Hindle for his help in editing the manuscript.

References

1. Nomura S, Sawada S (1955) J Phys Soc Jpn 10:108
2. Somiya Y, Bhalla AS, Cross LE (2001) Int J Inorg Mater 3:709
3. Kang DH, Kim HJ, Park JH, Yoon KH (2001) Mater Res Bull 36:265
4. Jain M, Majumder SB, Guo R, Bhalla AS, Katiyar RS (2002) Mater Lett 56:692
5. Zhang F, Karaki T, Adachi M (2005) Powder Technol 159:13
6. Leal SH, Escote MT, Pontes FM, Leite ER, Joya MR, Pizani PS, Longo E, Varela JA (2009) J Alloys Compd 475:940
7. Sen S, Choudhary RNP (2007) Appl Phys A 87:727
8. Zhou L, Zimmermann A, Zeng YP, Aldinger F (2004) J Mater Sci Mater Electron 15:145
9. Sumang R, Bongkarn T (2010) Key Eng Mater 421:243
10. Rivera I, Kumar A, Mendoza F, Katiyar RS (2008) Physica B 403:2423
11. Sumang R, Bongkarn T (2009) Funct Mater Lett 2:193
12. Amaranda L, Miclea C, Tanasoiu C (2002) J Eur Ceram Soc 22:1269
13. Bongkarn T, Rujijanagul G, Milne SJ (2005) Mater Lett 59:1200
14. Sumang R, Bongkarn T (2009) Ferroelectrics 383:57
15. Song Z, Gao J, Zhu X, Wang L, Fu X, Lin C (2001) J Mater Sci 36:4285. doi:10.1023/A:1017999223329
16. Udomporn A, Ananta S (2004) Mater Lett 58:1154
17. Tagawa H, Igarashi K (1986) J Am Ceram 69:310
18. Chen H, Yang C, Zhang J, Pei Y, Zhao Z (2009) J Alloys Compd 486:615
19. Powder Diffraction File No. 06-0452, International Center for Diffraction Data, Newton Square, PA, 2003
20. Powder Diffraction File No. 06-0634, International Center for Diffraction Data, Newton Square, PA, 2003
21. Vittayakorn N, Rujijanagul G, Tunkasiri T, Xiaoli T, Cann DP (2003) J Mater Res 18:2882
22. Chu SY, Chen TY, Tsai IT (2003) Integr Ferroelectr 58:1293
23. Yimnirun R, Tipakontitikul R, Ananta S (2006) Int J Mod Phys B 20:2415
24. Selbach SM, Tybell T, Einarsrud M, Grande T (2011) Appl Phys Lett 98:091912
25. Kong LB, Ma J, Huang H, Zhang RF (2002) J Alloy Compd 345:238
26. Zhang Y, Kuang A, Chan HLW (2003) Microelectr Engine 66:918